



HAL
open science

Real-time in-situ spectroscopic ellipsometry of GaSb nanostructures during sputtering: Identification of growth regimes

Ingar S. Nerbo, Sébastien Le Roy, Morten Kildemo, Elin Sondergard

► **To cite this version:**

Ingar S. Nerbo, Sébastien Le Roy, Morten Kildemo, Elin Sondergard. Real-time in-situ spectroscopic ellipsometry of GaSb nanostructures during sputtering: Identification of growth regimes. Applied Physics Letters, 2009, 94 (21), pp.213105. hal-00499356

HAL Id: hal-00499356

<https://hal.science/hal-00499356v1>

Submitted on 12 Jul 2010

HAL is a multi-disciplinary open access archive for the deposit and dissemination of scientific research documents, whether they are published or not. The documents may come from teaching and research institutions in France or abroad, or from public or private research centers.

L'archive ouverte pluridisciplinaire **HAL**, est destinée au dépôt et à la diffusion de documents scientifiques de niveau recherche, publiés ou non, émanant des établissements d'enseignement et de recherche français ou étrangers, des laboratoires publics ou privés.

Real-time in-situ spectroscopic ellipsometry of GaSb nanostructures during sputtering: Identification of growth regimes

I.S. Nerbø¹, S. Le Roy², M. Kildemo¹, E. Søndergård²

¹Physics Department, Norwegian University of Science and Technology (NTNU) NO-7491 Norway and

²UMR 125 Unit mixte CNRS/Saint-Gobain Laboratoire Surface du Verre et Interfaces

39 Quai Lucien Lefranc, F-93303 Aubervilliers Cedex, France

(Dated: February 12, 2009)

We demonstrate that in-situ spectroscopic ellipsometry can be used to measure the height evolution of nanostructures during low energy ion sputtering of GaSb. A graded anisotropic effective medium approximation is used to extract the height from the optical measurements. Two different growth regimes have been observed, first exponential, then followed by a linear regime. The linear regime is not expected by the traditional sputtering theories. The in-situ results correspond well to ex-situ AFM measurements.

PACS numbers: 81.07.-b, 07.60.Fs, 64.75.Yz

Self organized nanostructures open up for efficient and low-cost production of materials with new and interesting properties, with potential applications in electronics, optics and life sciences [1–4]. A major challenge for controlling and understanding growth processes for such structures is the characterization of nanometer sized structures. Traditional near field techniques such as atomic force microscopy (AFM), scanning electron microscopy and transmission electron microscopy, are time consuming and not suited for in-situ use. A fast observation technique compatible with vacuum chambers is necessary for studies of growth laws and their dependence on formation conditions. Grazing-incidence small-angle x-ray scattering (GISAXS) has been used for real time in-situ characterization of nanostructures during growth, with sub-nanometer sensitivity [5]. Unfortunately, this technique requires an intense well-collimated x-ray beam, typically provided by a synchrotron. Spectroscopic ellipsometry (SE) is on the other hand a much more accessible technique, based on measuring the change of polarization state of light, and ellipsometers can easily be mounted on most growth chambers. It is a much used technique for accurately measuring dielectric functions and the thickness of thin layers (see *e.g.* [6]), and for real-time monitoring of thin film growth (see *e.g.* [7–9]). Because of the wavelength range used, SE cannot determine the lateral size or ordering of nanostructures. However, by modeling the structures as a thin film the average height can be accurately determined. In this work we demonstrate the capability of SE to monitor the height evolution of nanostructures from real-time in-situ measurements. As an example of nanostructuring, we have studied low energy ion sputtering of GaSb, leading to high aspect ratio pillars. Such structures have interesting antireflective properties [10], and have recently been reported to have a formation process induced by nanoscale segregation of Ga [11], which could have interesting implications for the growth law.

The nanostructures were prepared on commercially available GaSb(100) wafers, in an ultra-high vacuum (UHV) chamber with a base pressure of 10^{-8} mbar.

The sputter gas was 300eV Ar⁺ with a flux of (0.017 ± 0.001) mA/scm². The ion incidence was normal to the sample surface, and all samples were sputtered at room temperature. A SE (MM16, Horiba Jobin Yvon) with a fast CCD spectrograph (spectral range 1.46–2.88eV) was used to do in-situ measurements during sputtering. A sketch of the setup is shown in Fig. 1

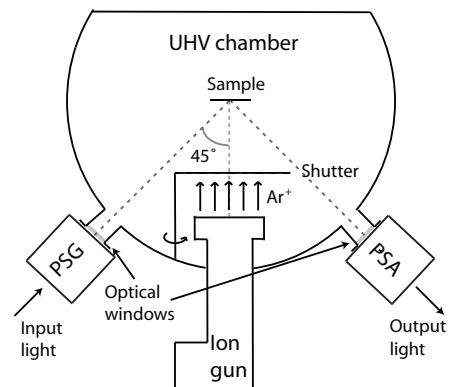


FIG. 1: Sketch of the experimental setup. The polarization state generator (PSG) and the polarization state analyzer (PSA) of the ellipsometer were mounted on two low-strain optical windows, giving a fixed angle of incidence of 45° on the sample.

A series of samples have been observed in-situ for different sputtering exposure times, ranging from 2 to 30 minutes. After sputtering the surfaces were characterized by AFM. Fig. 2 shows an image of a sample surface after sputtering, revealing disordered nanopillars with regular shape and size, which can be described as truncated cones (see inset Fig. 2)

In-situ SE spectra were recorded every 5th second during the sputtering, by measuring the ellipsometric intensities I_S and I_C . In case of no polarization coupling, the latter can be expressed as $I_S = \sin 2\Psi \sin \Delta$ and $I_C = \sin 2\Psi \cos \Delta$, where Ψ and Δ are defined from the ratio of the complex reflection coefficients $r_{pp}/r_{ss} = \tan \Psi \exp(i\Delta)$. Examples of SE measurements at dif-

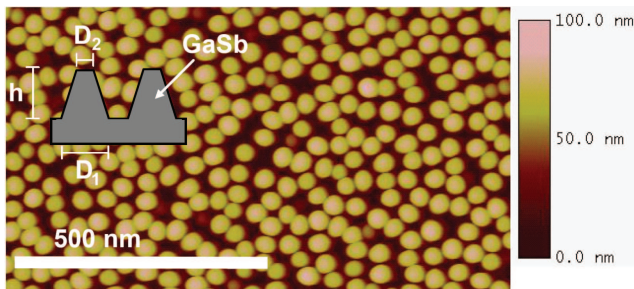


FIG. 2: (Color online) AFM image of the sample sputtered for 30 minutes. The inset is a sketch of the optical model, where h is the total height of the pillars, D_1 and D_2 are the bottom and top relative diameters.

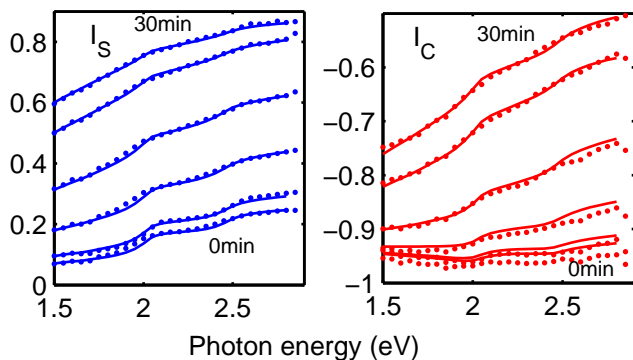


FIG. 3: (Color online) In-situ SE measurements (dots) of a sample at different stages in the formation process (after 0 (bottom curves), 1, 2, 3, 10 and 30 (top curves) minutes of sputtering), together with fitted effective medium models (solid lines).

ferent stages in the sputtering process are presented in Fig. 3. The surface structuration has a strong impact on the optical properties of the surface, indicating that SE is highly sensitive to such structures.

In a previous publication we demonstrated that the height of such nanostructures can be found by ex-situ ellipsometry [10], through effective medium modeling of the optical properties. The same model have been used to simulate the in-situ SE measurements, simplified by neglecting the oxide coating since the samples are measured in vacuum. The effective medium approximation is valid as long as the lateral dimension of the structures are sufficiently smaller than the wavelength of light. The effective dielectric function is calculated by treating the pillars as a stack of cylinders of GaSb with decreasing radius, surrounded by void. The effective dielectric function for each layer is found by using a generalized Bruggeman effective medium equation for ellipsoidal inclusions [12]

$$f_{GaSb} \frac{\epsilon_{GaSb} - \epsilon_{ii}}{\epsilon_{ii} + L_i(\epsilon_{GaSb} - \epsilon_{ii})} + f_v \frac{\epsilon_v - \epsilon_{ii}}{\epsilon_{ii} + L_i(\epsilon_v - \epsilon_{ii})} = 0, (1)$$

where f and ϵ denote the filling factors and complex di-

TABLE I: Comparison between in-situ SE results and ex-situ AFM measurements. h_{SE} and h_{AFM} are the heights found from SE and AFM, K_{AFM} is the mean nearest neighbor distance as estimated from AFM.

time	100s	2min	3min	5min	10min	30min
h_{SE} (nm)	19	27	38	48	57	83
h_{AFM} (nm)	22	26	35	46	55	82
K_{AFM} (nm)	39	41	43	41	45	51

electric functions, respectively, with the subscript $GaSb$ referring to the crystalline core, and v to the surrounding void. L_i denotes the depolarization factor in direction i (along a principal axis of the structure) and ϵ_{ii} is the effective dielectric function in direction i . For cylindrical inclusions, $L_{||} = 0.5$ parallel to the mean surface, and $L_{\perp} = 0$ perpendicular to the mean surface. This gives a uniaxial anisotropic material with the optic axis normal to the mean surface. In this case there is no polarization coupling ($r_{ps} = r_{sp} = 0$). Reflection coefficients for a stack of anisotropic layers have been calculated by an implementation of Schubert's algorithm [13], based on Berreman's 4×4 differential matrices [14].

Three parameters in the model have been fitted to the experimental measurements by minimizing a χ^2 function, as reported in Ref. [10] These parameters are the total height h of all layers, and the relative effective diameters D_1 and D_2 of the bottom and top cylinder, respectively (see inset Fig. 2). The diameters of the cylinders in intermediate layers decrease linearly from D_1 to D_2 . The diameters have been normalized to the nearest neighbor distance, since only volume filling factors affect the effective medium. The filling factors have been calculated for hexagonal ordering.

The height inferred from the in-situ SE measurements are compared to AFM height measurements in Table I, together with the lateral dimensions found by AFM. The two heights are in good correspondence for all the samples. From Monte Carlo simulations and the observed noise level, the dynamical sensitivity of the height derived from SE has been estimated to be less than 1nm. Finding the mean height of this kind of densely packed high-aspect ratio structures from AFM measurements is challenging, as images of these surfaces are very sensitive to tip effects. To account for the AFM tip not always reaching the bottom between closely packed pillars, the height of each top have been calculated in relation to a local minimum within a certain distance (d) from the top. The mean height calculated this way increase strongly with d as the distance is shorter than the mean bottom pillar radius. Then it saturates, and the mean height found then is a good approximation to real mean pillar height. This saturation distance corresponds well to half the mean nearest neighbor separation as estimated by AFM.

The height evolution of the samples during sputtering is derived from the SE measurements, and presented

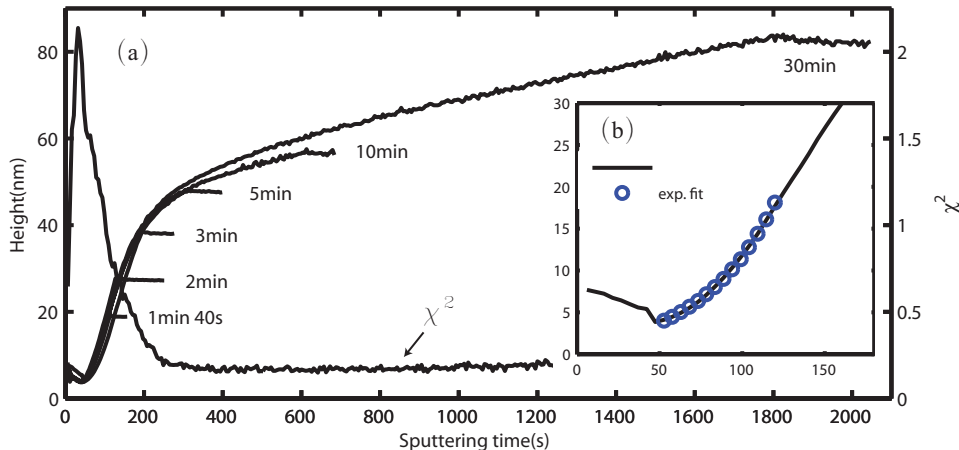


FIG. 4: (Color online) (a) Height evolution of GaSb nanopillars during low energy ion sputtering, for various ion beam exposure times, together with the χ^2 error function for the sample sputtered 30min. (b) Initial growth stage of the sample sputtered for 30 minutes.

in Fig. 4. The evolution of the different samples is observed to be very reproducible. Initially the GaSb wafers are covered by an approximately 7nm thick oxide layer, which will be removed at the initial stage of sputtering. In this stage the effective medium model described above is not valid, but still shows a decrease in height, corresponding to removal of oxide and possibly smoothing of the surface. After about 1 minute the height of the structure starts to increase at an exponential rate of 0.0225s^{-1} , lasting about 1 minute. The growth is then followed by a transition stage, until it becomes clearly linear after approximately 6 or 7 minutes of sputtering, with a growth rate of 0.019nm/s . No growth saturation is observed within 30 minutes. The average deviation from a linear fit for the last 15 minutes of sputtering is 0.3nm. The mean nearest neighbor distance estimated from the AFM measurements seem to be unchanged for the first 5 minutes of sputtering, and then to increase slowly after the transition to linear growth, with a total increase of approximately 10nm after 30 minutes.

The initial exponential growth of the structure during sputtering can be explained by Bradley and Harper's (BH) theory [15], where the growth is due to competition between curvature dependent sputtering yield [16] and diffusion processes. Non-linear extensions of the BH model

have been performed to describe growth saturation and hexagonal ordering of the structure [17, 18], but a linear regime has never been predicted for the growth. Le Roy *et al.* [11] have ascribed the growth to gallium segregation. Gallium rich zones will act as a sputter shield, and could account for the linear regime.

SE proves to be a sensitive tool for in-situ characterization of GaSb nanostructures, produced by low energy ion sputtering. The method, in-situ SE combined with appropriate modeling, gives results expected to be comparable to GISAXS synchrotron measurements, but with a table top setup that could easily be adapted to most growth chamber. The method has given new insight in the formation process of such structures, and opens up for an effective way to study the dependence of the structure growth on formation parameters (such as temperature, ion flux and energy). Such studies would be too time consuming and inaccurate if performed by AFM or electron microscopy methods. The method should be transferable to similar structures of different materials, formed by different processes.

Acknowledgements: We are thankful to Horiba Jobin Yvon for help with adapting the ellipsometer for in-situ use.

-
- [1] L. Samuelson, *Mater. Today* **6**, 22 (2003).
 [2] W. Wu, *Appl. Phys. Lett.* **90**, 063107 (2007).
 [3] A. Lafuma and D. Quere, *Nature Mater.* **2**, 457 (2003).
 [4] S. J. Wilson and M. C. Hutly, *J. Mod. Opt.* **29**, 993 (1982).
 [5] G. Renaud *et al.*, *Science* **300**, 1416 (2003).
 [6] R. M. A. Azzam and N. M. Bashara, *Ellipsometry and Polarized Light*, NORTH-HOLLAND, 1987.
 [7] W. M. Duncan and S. A. Henck, *Appl. Surf. Sci.* **63**, 9 (1993).
 [8] R. W. Collins *et al.*, *Thin Solid Films* **313-314**, 18 (1998).
 [9] M. Kildemo, R. Brenot, and B. Drévilion, *Appl. Opt.* **37**, 5145 (1998).
 [10] I. S. Nerbø *et al.*, *Appl. Opt.* **47**, 5130 (2008).
 [11] S. Le Roy, N. Brun, A. Lelarge, E. Søndergård, and E. Barthel, Ga segregation initiates formation of gasb pillars during ion sputtering, (In submission), 2009.

- [12] J. E. Spanier and I. P. Herman, Phys. Rev. B **61**, 10437 (2000).
- [13] M. Schubert, Phys. Rev. B **53**, 4265 (1996).
- [14] D. W. Berreman, J. Opt. Soc. Am. **62**, 502 (1972).
- [15] R. M. Bradley and J. M. E. Harper, J. Vacu. Sci. Tech. A: Vacuum, Surfaces and Films **6**, 2390 (1988).
- [16] P. Sigmund, Phys. Rev. **184**, 383 (1969).
- [17] M. Castro, R. Cuerno, L. Vázquez, and R. Gago, Phys. Rev. Lett. **94**, 016102 (2005).
- [18] S. Fucsko et al., Science **285**, 1551 (1999).